IOP Publishing Journal of Physics B: Atomic, Molecular and Optical Physics
J. Phys. B: At. Mol. Opt. Phys. **47** (2014) 215301 (5pp) doi:10.1088/0953-4075/47/21/215301

A linear array of 11 double-loop microtraps for ultracold atoms

B Jian and W A van Wijngaarden

Physics Department, Petrie Building, York University, 4700 Keele St., Toronto, ON, M3J 1P3, Canada

E-mail: wlaser@yorku.ca

Received 23 July 2014, revised 19 August 2014
Accepted for publication 21 August 2014
Published 15 October 2014

Abstract

A linear array of 11 closely spaced microtraps was demonstrated. Each microtrap was created using the magnetic field generated by two concentric circular wire loops having radii of 60 and 132 μm carrying oppositely oriented currents as well as a bias magnetic field oriented perpendicular to the atom chip surface containing the microwire loops. ^{87}Rb atoms were initially cooled using either a surface magneto-optical trap (MOT) or a far off resonance optical dipole trap (FORT) created using an infrared laser directed along the microtrap array axis. The microtrap current was turned on and over 12 000 atoms were loaded into each microtrap. The advantage of FORT loading was that the 11 microtraps were about equally populated and the microtrapped atom temperature of 11 μK was one quarter of that obtained using the MOT.

Keywords: magnetic microtrap array, ultracold atoms, laser cooling and trapping

(Some figures may appear in colour only in the online journal)

1. Introduction

Considerable progress has been made to develop magnetic microtraps of ultracold atoms in the last decade [1–4]. An important advantage when compared to traditional macroscopic traps is that microtrapped atoms experience similar magnetic field strengths and larger field gradients that are generated using orders of magnitude smaller currents. A number of interesting applications of microtraps have been demonstrated in such diverse fields as Bose–Einstein condensation [2, 5], surface sensing [6], atom interferometry [7] and quantum information processing [8].

Arrays of ultracold atoms have recently been generated using optical as well as magnetic microtraps. An optical trap array was created using specialized optics consisting of many microlenses to produce multiple foci of an infrared laser beam [9, 10]. Magnetic microtrap arrays were produced using the permanent magnetic field of a surface magnetic film [11, 12]. A long term objective of both optical and magnetic microtrap arrays is to study quantum information processing.

Our group recently demonstrated a magnetic microtrap generated by the fields produced by two concentric circular loops carrying oppositely oriented currents [13–15]. The current can be adjusted thereby controlling the trap potential which is not possible using a permanent magnetic film. The addition of a bias magnetic field oriented perpendicular to the plane of the microwire loops increased the trap depth and also permitted precise adjustment of the microtrapped atom cloud position relative to the atom chip surface. An atom chip was demonstrated consisting of three microtraps spaced 1.5 mm apart. The inner and outer radii of the microtrap loops were 300 and 660 μm, respectively. About 10^5 atoms, initially prepared in either a magneto-optical trap (MOT) or in a far off resonance optical dipole trap (FORT), could be loaded into two of the microtraps. The temperature of the microtrapped atom cloud was measured to be as low as 40 μK.

This paper reports the demonstration of a linear array of 11 closely spaced microtraps as is shown in figure 1. Each trap consists of two microwire loops having radii $r_1 = 60$ and $r_2 = 132$ μm and have oppositely oriented currents I. This generates a three dimensional trap centered at a position $z = 1.15r_1$, where z points in the vertical downward direction perpendicular to the x–y plane containing the microwire loops as is shown in figure 1 (b)–(d) [14, 16]. The addition of a bias field B_{zbias} in the z direction increases the trap depth to a maximum when $B_{\mathrm{zbias}} = 1.62B_0$, where $B_0 = \frac{\mu_0 I}{4\pi r_1}$. For the case of $I = 0.5$ A and $B_0 = 8.67$ G, a ^{87}Rb atom in the $m_F = 2$ Zeeman sublevel of the $F = 2$ ground state hyperfine level experiences a maximum trap depth of 1.2 mK. The bias

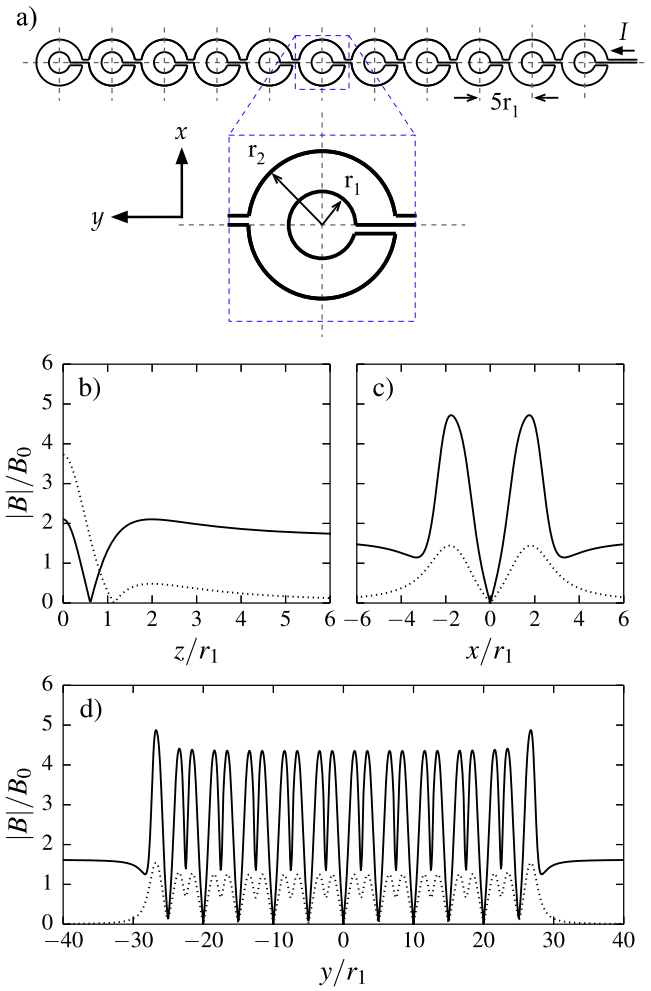

Figure 1. Microtrap array configuration. Each of the 11 microtraps shown in (a) consists of two concentric microwire loops of radii $r_1 = 60\ \mu$m and $r_2 = 2.2r_1$. The trap centers are located a distance $5r_1$ apart. The origin of the coordinate system is at the center of the middle microtrap located at the chip surface where $z = 0$. The dependence of the magnetic field magnitude calculated along the z, x and y directions from the center of the middle microtrap are shown in (b)–(d) for the case of zero bias field (dashed line) and $B_{\text{zbias}} = 1.62B_0$ (solid line).

field also shifts the trap minimum toward the chip surface from $z = 1.15r_1$ when $B_{\text{zbias}} = 0$ to $z = 0.61r_1$, when $B_{\text{zbias}} = 1.62B_0$.

This paper describes how to load the microtrap array either directly from a MOT or from a FORT created using an infrared laser aligned along the microtrap array axis. The dependence of the microtrap populations on the bias field is examined and various characteristics of the trapped atoms such as the temperature and lifetime are determined.

2. Apparatus and procedure

The apparatus is similar to that described in our previous work and is therefore only briefly discussed here [14, 15]. The atom chip was housed in a pyrex cell that was pumped down to a pressure of 10^{-10} torr using a combination titanium sublimation and ion pump. The atom chip was attached to a copper block heat sink using thermally conductive epoxy EpoTek H77. The atom chip, fabricated by Canadian Microelectronics Corp., consisted of a 0.5 mm thick silicon wafer onto which first a 100 nm silicon nitride insulating layer was deposited followed by a 4 μm Cu layer. The microtrap array wire pattern shown in figure 1(a) was etched into the Cu surface. The resulting microwires had a width of 7 μm and were separated by a 5 μm insulating gap from the remainder of the Cu surface. The resistance of the circuit was measured to be 14 Ω in excellent agreement with the calculated value.

Ultracold ^{87}Rb atoms were produced using standard laser cooling techniques [17–19]. A surface MOT was generated by reflecting laser beams from the atom chip surface which had a reflectivity greater than 90% at 780 nm. Two coils, external to the vacuum chamber and centered about a point 2 mm below the atom chip, generated a quadrupole magnetic field having a gradient along their axial direction of 14 G cm^{-1}. The trap laser beam was detuned 14 MHz below the $F = 2 \rightarrow F' = 3$ cycling transition of the ^{87}Rb D2 line and had an intensity of 40 mW cm^{-2}, where F and F' denote the hyperfine levels of the $5S_{1/2}$ ground state and $5P_{3/2}$ excited state, respectively. The repump laser was frequency locked to the $F = 1 \rightarrow F' = 2$ transition and had an intensity of 2 mW cm^{-2}. The resulting atom cloud was studied by monitoring the transmission of a probe laser through the ultracold atom clouds using a CCD camera. The 50 μW probe laser beam propagated parallel to the atom chip surface along the x direction. It was frequency locked to the cycling transition of the D2 line and had a beam area of about 1 cm^2. Approximately 2×10^7 atoms could be loaded into the MOT in 6 s.

The procedure to load the microtrap array directly from the MOT is given in table 1. The MOT cloud was first compressed (CMOT) by increasing the magnetic field gradient from 14 to 35 G cm^{-1}. During this time the trap laser detuning was increased to 30 MHz and the repump laser intensity was reduced by a factor of two to minimize atom heating. Small magnetic fields of up to 2 G were applied along the x, y and z directions to shift the MOT cloud position to beneath the middle microtrap of the array. Next, all magnetic fields were switched off and the trap laser detuning was increased to 50 MHz to further cool the atoms. Typically, about 10^7 atoms remained in the MOT after this 8 ms optical molasses stage. The temperature of $40 \pm 3\ \mu$K was determined by studying the temporal expansion of the atom cloud [17]. Next, the atoms were optically pumped to the $m_F = 2$ magnetically trapped Zeeman sublevel of the $F = 2$ ground state hyperfine level using a 1 ms circularly polarized laser beam resonant with the $F = 2 \rightarrow F' = 2$ transition of the D2 line. The 80 μW optical pumping laser beam overlapped with a small fraction of the repump laser beam to avoid accumulation of atoms in the $F = 1$ ground state hyperfine level. A magnetic field of 2.5 G was applied along the laser propagation direction to define the quantization axis. Optical pumping transferred more than 90% of the atoms into the $m_F = 2$ Zeeman sublevel of the $F = 2$ ground state hyperfine

level. The microtrap was then turned on by suddenly increasing the atom chip current to 0.5 A as well as the B_{zbias} field.

Table 1 also gives the procedure to load the microtrap array from the FORT. The FORT was created by focussing a 15 W laser operating at 1064 nm beam into a spot measured to have a beam waist radius of 34 μm. The infrared laser beam propagated along the y direction beneath the atom chip. The MOT cloud was compressed and atoms were cooled using optical molasses as described in the previous paragraph. Two differences were that the repump laser power was reduced to 40 μW and the durations of the CMOT and optical molasses stages were increased to 140 and 20 ms, respectively. This was done to reduce the number of spin exchange and or photoassociative collisions between atoms in the two hyperfine ground state levels that have been found to cause a significant loss of trapped atoms [20, 21]. The resulting FORT consisted of 7.5×10^5 atoms occupying the $F = 1$ ground state hyperfine level. A FORT holding time of 30 ms allowed for the dispersal of atoms not loaded into the FORT. The temperature of atoms in the FORT was measured to be 130 ± 10 μK. Next, the microtrap array was turned on over 20 ms by linearly increasing both the atom chip current to 0.5 A and the bias magnetic field B_{zbias}. The FORT laser power was then decreased to zero in 50 ms which was previously found to optimize the number of atoms loaded into the microtrap array [15].

Atoms were held in the microtrap array for up to 400 ms after both MOT and FORT loading. A 50 μs probe laser pulse was then incident on the atom clouds. A variable probe delay time after the micotrap was suddenly switched off permitted the measurement of the temporal expansion of the atom cloud to determine its temperature. For the case of microtrap loading from the FORT, the trapped atoms were in the $m_F = -1$ Zeeman sublevel of the $F = 1$ ground state hyperfine level. The atoms were then probed by overlapping about 100 μW of repump laser light with the probe laser beam.

3. Results

Figure 2 shows the microtrapped atoms loaded from the surface MOT. The images shown in figures 2(a) and (b) are the average of 15 images taken using B_{zbias} of 8 G. Individual microtrap populations are visible, although adjacent microtrapped clouds overlap due to diffraction of the probe beam with the atom chip surface [22]. The distribution of atoms in the microtrap array depended on B_{yshift} which shifted the position of the MOT along the y direction. The MOT cloud, centered 0.4 mm below the atom chip surface, had more than 50% of its atoms inside a spherical shape having a diameter of 1.5 mm with its top part truncated by the atom chip. The MOT diameter was less than the 3 mm length of the microtrap array. Hence, atoms were predominantly loaded into the right half of the microtrap array when $B_{\text{yshift}} = 0$ as shown in figure 2(a). For the case when $B_{\text{yshift}} = 0.5$ G, a total of

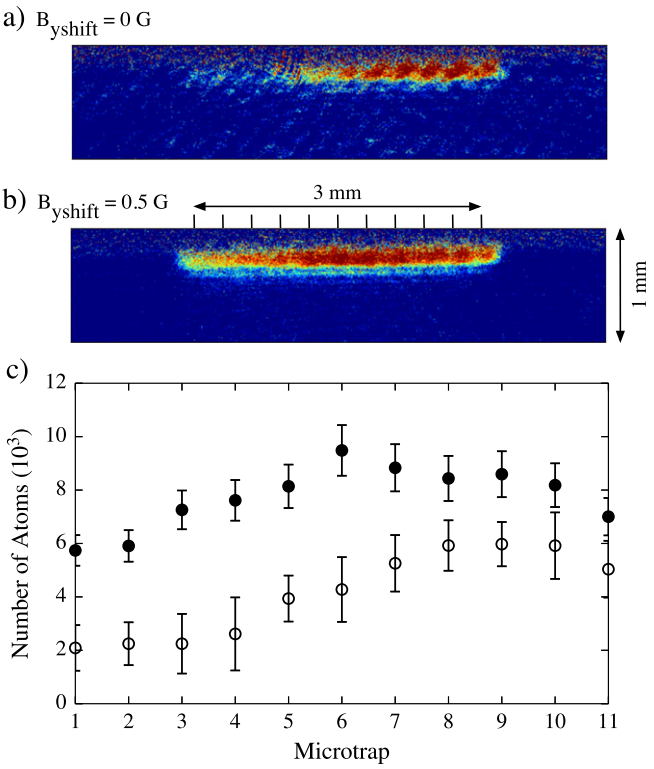

Figure 2. Images of the atoms loaded into the microtrap array using $B_{\text{zbias}} = 8$ G with (a) $B_{\text{yshift}} = 0$ and (b) $B_{\text{yshift}} = 0.5$ G. The ticks on the top of (b) indicate the positions of the microtrap centers. (c) Number of atoms loaded into the individual microtraps counted from left to right for $B_{\text{yshift}} = 0$ (open circle) and $B_{\text{yshift}} = 0.5$ (solid circle).

8.5×10^4 atoms were loaded into the microtrap array with an average of 7800 atoms in each microtrap.

The dependence of the microtrapped atom number on the bias magnetic field B_{zbias} is shown in figure 3. Each data point is the average of five separate measurements and the error bar equals one standard deviation. Relatively few atoms were trapped at low values of the bias field because the trap depth was small as illustrated in figure 1. The maximum number of trapped atoms occurred at a bias field of 8 G. This was less than the calculated value of 14 G (1.62 B_0) that maximizes the trap depth. An increase of the bias field from 0 to 20 G also shifts the calculated microtrap position from 69 to 28 μm below the chip surface. The image resolution was insufficient to accurately measure this shift. Hence, the trap volume was limited by the proximity of the chip surface, which limited the number of atoms in the microtrap.

Figure 4 shows the number of atoms loaded into the microtraps from the FORT. The FORT was aligned along the microtrap array axis and was positioned 65 ± 15 μm below the microtrap array as shown in figure 4(a). The resulting microtraps were nearly equally loaded with the exception of the outermost traps where the FORT cloud was less dense. The total number of atoms loaded into the microtrap array was 1.3×10^5 with an average of 1.2×10^4 atoms in each microtrap.

Table 1. Typical timing sequence to load atoms into the microtrap array from a surface MOT and a FORT.

Surface MOT loading	Interval	FORT loading	Interval
MOT loading	6 s	MOT loading	6 s
CMOT	50 ms	CMOT+ FORT loading	120 ms
Optical molasses	8 ms	FORT + optical molasses	20 ms
Optical pumping	1 ms	FORT holding	30 ms
Microtrap holding	30–400 ms	Microtrap ramp on	20 ms
Probe delay	0.1–2.5 ms	Microtrap holding + FORT ramp down	50 ms
Probing	50 μs	Microtrap holding	30–400 ms
		Probe delay	0.1–2.5 ms
		Probing	50 μs

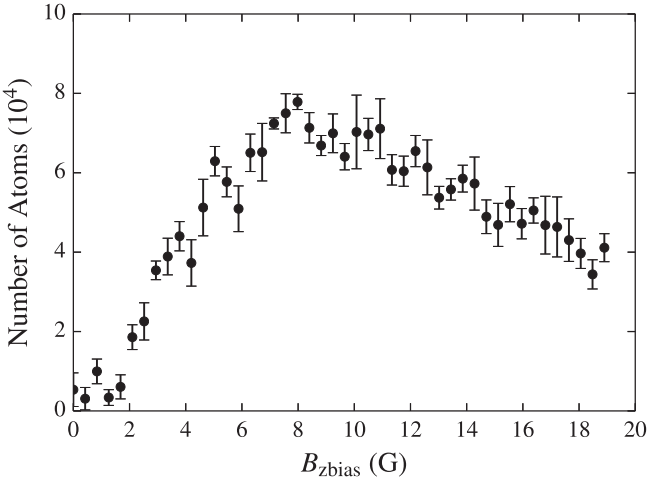

Figure 3. Total number of atoms loaded into the 11 microtraps directly from the surface MOT as a function of the bias magnetic field B_{zbias}.

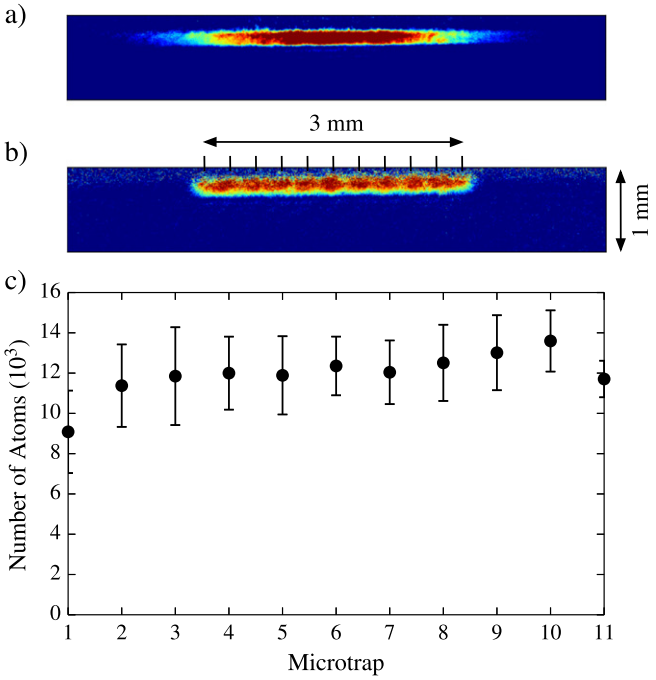

Figure 4. (a) Image of the atoms trapped in the FORT which was loaded from the surface MOT. The FORT was positioned 65 ± 15 μm beneath the atom chip surface. (b) Image of atoms in the microtrap array loaded using B_{zbias} = 3 G from the FORT. The ticks on the top of (b) indicate the positions of the individual microtrap centers. (c) Number of atoms loaded into the individual microtraps counted from left to right.

The dependence of the microtrapped atom number loaded from the FORT on the bias magnetic field B_{zbias} is shown in figure 5. The number of atoms increased sharply when the bias field was applied because this increased the trap depth. The maximum trapped atom number occurred at a bias field of about 2.5 G. At higher bias fields, the number of trapped atoms was reduced as the microtrap position shifted away from the FORT and towards the atom chip surface. Indeed, the number of trapped atoms was reduced by 50% when the laser was expressly positioned 100 ± 15 μm below the atom chip. However, the bias field of 2.5 G that optimized the trapped atom number was unchanged.

The atom temperature was determined by monitoring the expansion of the atom cloud in the vertical direction after the atom chip current and B_{zbias} were turned off. A temperature of 40 ± 4 μK was found for atoms loaded into the microtrap in the $F = 2$, $m_F = 2$ Zeeman sublevel from the MOT whereas atoms loaded from the FORT in the $F = 1$, $m_F = -1$ Zeeman sublevel had a temperature of only 11 ± 2 μK. The lower temperature achieved using FORT loading was consistent with our previous experiment that used a larger microtrap [15]. It arises because evaporative cooling is facilitated when the FORT laser power is ramped down [23–25].

The lifetime of the atoms was measured by varying the microtrap array holding time to be 304 ± 34 and 293 ± 30 ms for loading from the MOT and the FORT, respectively. This lifetime was limited by collisions with the background gases [25] as well as by Majorana spin flips [26].

4. Conclusions

This experiment successfully demonstrated how to load a one dimensional array of 11 microtraps either directly from a surface MOT or from a FORT. The advantage of using FORT loading is that the infrared laser beam can be conveniently aligned with the microtrap axis resulting in a population distribution among the microtraps that is quite uniform. A

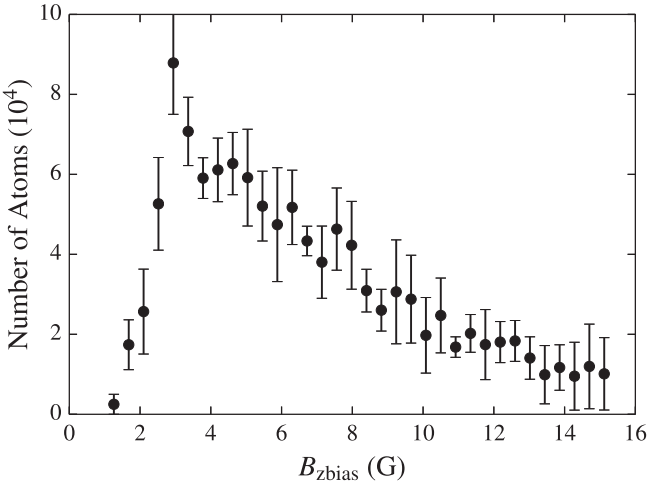

Figure 5. Total number of atoms loaded into the microtrap array from the FORT as a function of the bias magnetic field B_{zbias}.

total of 1.3×10^5 atoms could be loaded into the microtrap with an average of over 12 000 atoms in each microtrap.

The microtrap consisted of two current loops with the inner loop radius $r_1 = 60\,\mu$m. This is five times smaller than our previous work that loaded 1×10^5 atoms into a single double-loop microtrap. The atom temperature was four times larger than the 11 μK found in this work. The atom cloud radius in that earlier experiment was measured to be half the inner loop radius of 300 μm. This was used to estimate the peak trap density to be 1×10^{10} atoms cm^{-3}. It was not possible to accurately determine the atom cloud size in the present experiment as mentioned earlier. However, assuming the trap volume scales as r_1^3, the atom density of the present microtrap is estimated to be $\approx 1 \times 10^{11}$ atoms cm^{-3}.

It should be possible to further reduce the microtrap size as the present microtrap used a current of 0.5 A and no degradation of the atom chip caused by resistive heating was evident. The trap depth scales as the current divided by r_1. For example, a reduction of r_1 by an additional factor of 5 to 12 μm would require only a current of 100 mA to achieve the same trap depth. The number of microtrapped atoms would be reduced but the atom density can be expected to increase until it is limited by collisions between ultracold atoms and Majorana transitions [26]. More sensitive imaging techniques such as fluorescence detection would be required to detect these smaller numbers of atoms [27, 28]. This would also facilitate improved detection of the size of the atom cloud and its position relative to the chip surface. An important advantage of our microtrap design is that unlike microtraps that rely on permanent magnetic films, the surface of the atom chip immediately above the ultracold atom cloud is available to mount a diode laser or an optical fiber. This would facilitate addressability of individual microtraps which is essential to develop quantum processing capabilities. Hence, a one or even two dimensional array of double-loop microtraps has significant potential as a platform for experiments investigating ultracold atoms.

Acknowledgments

The authors wish to thank the Natural Science and Engineering Research Council of Canada for financial support. B Jian gratefully acknowledges York University for providing the Provost Scholarship.

References

[1] Weinstein J D and Libbrecht K G 1995 *Phys. Rev.* A **52** 4004
[2] Hänsel W, Hommelhoff P, Hänsch T W and Reichel J 2001 *Nature* **413** 498
[3] Folman R, Krüger P, Schmiedmayer J, Denschlag J and Henkel C 2002 *Adv. At. Mol. Opt. Phys.* **48** 263
[4] Fortágh J and Zimmermann C 2007 *Rev. Mod. Phys.* **79** 235
[5] Ott H, Fortágh J, Schlotterbeck G, Grossmann A and Zimmermann C 2001 *Phys. Rev. Lett.* **87** 230401
[6] Gierling M, Schneeweiss P, Visanescu G, Federsel P, Haffner M, Kern D P, Judd T E, Günther A and Fortágh J 2011 *Nat. Nanotechnology* **6** 446
[7] Wang Y-J, Anderson D Z, Bright V M, Cornell E A, Diot Q, Kishimoto T, Prentiss M, Saravanan R A, Segal S R and Wu S 2005 *Phys. Rev. Lett.* **94** 090405
[8] Treutlein P, Hommelhoff P, Steinmetz T, Hänsch T W and Reichel J 2004 *Phys. Rev. Lett.* **92** 203005
[9] Knoernschild C, Zhang X L, Isenhower L, Gill A T, Lu F P, Saffman M and Kim J 2010 *Appl. Phys. Lett.* **97** 134101
[10] Lichtman M, Piotrowicz M, Xia T, Isenhower L and Saffman M 2014 *24th Int. Conf. on Atomic Physics* p 319
[11] Leung V Y F *et al* 2014 *Rev. Sci. Instrum.* **85** 053102
[12] Jose S, Surendran P, Wang Y, Herrera I, Krzemien L, Whitlock S, McLean R, Sidorov A and Hannaford P 2014 *Phys. Rev.* A **89** 051602(R)
[13] van Wijngaarden W A 2005 *Can. J. Phys.* **83** 671
[14] Jian B and van Wijngaarden W A 2013 *J. Opt. Soc. Am.* B **30** 238
[15] Jian B and van Wijngaarden W A 2014 *Appl. Phys.* B **115** 61
[16] Jian B 2014 *PhD Thesis* York University
[17] Metcalf H J and van der Straten P 1999 *Laser Cooling and Trapping* (New York: Springer)
[18] Pethick C J and Smith H 2008 *Bose–Einstein Condensation in Dilute Gases* (Cambridge: Cambridge University Press)
[19] Lu B and van Wijngaarden W A 2004 *Can. J. Phys.* **82** 81
[20] Kuppens S J M, Corwin K L, Miller K W, Chupp T E and Wieman C E 2000 *Phys. Rev.* A **62** 013406
[21] Walker T and Feng P 1997 *Adv. At. Mol. Opt. Phys.* **34** 125
[22] Shengwang Du 2005 *PhD Thesis* University of Colorado at Boulder
[23] Adams C S, Lee H J, Davidson N, Kasevich M and Chu S 1995 *Phys. Rev. Lett.* **74** 3577
[24] Cano D, Hattermann H, Kasch B, Zimmermann C, Kleiner R, Koelle D and Fortágh J 2011 *Eur. Phys. J.* D **63** 17
[25] van Dongen J, Hu Z, Clement D, Dufour G, Booth J L and Madison K W 2011 *Phys. Rev.* A **84** 022708
[26] Petrich W, Anderson M H, Ensher J R and Cornell E A 1995 *Phys. Rev. Lett.* **74** 3352
[27] Teper I, Lin Y-J and Vuletić V 2006 *Phys. Rev. Lett.* **97** 023002
[28] Ockeloen C F, Tauschinsky A F, Spreeuw R J C and Whitlock S 2010 *Phys. Rev.* A **82** 061606